ORIGINAL ARTICLE

Ground-motion networks in the Groningen field: usability and consistency of surface recordings

Michail Ntinalexis (iD) · **Julian J. Bommer** (iD) · **Elmer Ruigrok** (iD) · **Benjamin Edwards** (iD) · **Rui Pinho** (iD) ·
Bernard Dost (iD) · **António A. Correia** (iD) · **Jeroen Uilenreef** · **Peter J. Stafford** (iD) · **Jan van Elk**

Abstract Several strong-motion networks have been installed in the Groningen gas field in the Netherlands to record ground motions associated with induced earthquakes. There are now more than 450 permanent surface accelerographs plus a mobile array of 450 instruments, which, in addition to many instrumented boreholes, yield a wealth of data. The database of recordings has

Article Highlights
• Description of several ground-motion networks operating to record induced earthquakes in the Groningen gas field.
• Comparisons of the recordings and how these identified and resolved a configuration issue with one of the networks.
• Use of shake table tests on full-scale models to determine usability of recordings from wall-mounted accelerographs.

M. Ntinalexis
Independent Engineering Consultant, London, UK
e-mail: michail.ntinalexis10@alumni.imperial.ac.uk

J. J. Bommer (✉) · P. J. Stafford
Civil & Environmental Engineering, Imperial College London, Skempton Building, South Kensington Campus, London SW7 2AZ, UK
e-mail: j.bommer@imperial.ac.uk

P. J. Stafford
e-mail: p.stafford@imperial.ac.uk

E. Ruigrok · B. Dost
Royal Netherlands Meteorological Institute (KNMI), Utrechtseweg 297 3731GA, De Bilt, The Netherlands

E. Ruigrok
e-mail: elmer.ruigrok@knmi.nl

B. Dost
e-mail: bernard.dost@knmi.nl

B. Edwards
Department of Earth, Ocean and Ecological Sciences, University of Liverpool, 4 Brownlow Street, Liverpool L69 3GP, UK
e-mail: ben.edwards@liverpool.ac.uk

R. Pinho
Civil Engineering & Architecture, University of Pavia, Via Ferrata 1, 27100 Pavia, Italy
e-mail: rui.pinho@unipv.it

A. A. Correia
National Laboratory for Civil Engineering (LNEC), Av. do Brasil 101, 1700-066 Lisbon, Portugal
e-mail: aacorreia@lnec.pt

J. Uilenreef · J. van Elk
Nederlandse Aardolie Maatschappij B.V. (NAM), Schepersmaat, 2, 9405 TAAssen, The Netherlands

J. Uilenreef
e-mail: jeroen.uilenreef@shell.com

J. van Elk
e-mail: jan.van-elk@shell.com

been of fundamental importance to the development of ground-motion models that form a key element of the seismic hazard and risk estimations for the field. In order to maximise the benefit that can be derived from these recordings, this study evaluates the usability of the recordings from the different networks, in general terms and specifically with regards to the frequency ranges with acceptable signal-to-noise ratios. The study also explores the consistency among the recordings from the different networks, highlighting in particular how a configuration error was identified and resolved. The largest accelerograph network consists of instruments housed in buildings around the field, frequently installed on the lower parts of walls rather than on the floor. A series of experiments were conducted, using additional instruments installed adjacent to these buildings and replicating the installation configuration in full-scale shake table tests, to identify the degree to which structural response contaminated the recordings. The general finding of these efforts was that for PGV and oscillator periods above 0.1 s, the response spectral ordinates from these recordings can be used with confidence.

Keywords Induced seismicity · Ground-motion recording · Recording networks · Accelerographs

1 Introduction

The Groningen gas field, the largest in Western Europe, was discovered in 1959. Gas production from the field began in 1963 and the reservoir is now estimated to be about three-quarters depleted. The resulting compaction of the reservoir, which is within a sandstone layer at a depth of about 3 km, has reactivated geological faults in the field leading to induced seismicity. The first production-related earthquake in the Groningen field was detected in 1991 and many events of local magnitude greater than M_L 2.0 have occurred in the field since. The largest events to date were an earthquake of M_L 3.5 in August 2006 and another of M_L 3.6 in August 2012. The impact and aftermath of the latter event heightened regulatory and public concern

regarding the potential risk due to induced seismicity in the field. A key component of the response of the field operator, Nederlandse Aardolie Maatschappij(NAM), to this situation has been the development of probabilistic seismic hazard and risk models to quantify the potential impact (van Elk et al. 2017). The seismic risk model, which is capable of estimating the impact of production changes and of structural strengthening of the exposed buildings, has been designed to provide a basis for informed decision-making regarding appropriate mitigation measures (van Elk et al. 2019).

A core element of the hazard and risk modelling is a ground-motion prediction model to link the model for earthquake occurrence with the potential impact on the build environment via fragility functions (Crowley et al. 2017, 2019). The development of the ground-motion model (GMM) for induced earthquakes in the Groningen field has benefited enormously from the data retrieved from various recording networks that have been installed in the region. Strong-motion recordings obtained from instruments in the field highlighted the necessity of developing a bespoke GMM for Groningen (Bourne et al. 2015; Bommer et al. 2016). The basic framework of the GMM are equations for predicting motions at a rock horizon located at a depth of about 800 m combined with frequency-dependent non-linear amplification factors assigned to zones defined over the field as well as a 5-km onshore buffer zone (Bommer et al. 2017b). The equations predicting accelerations at the reference rock horizon are obtained from regressions on the output from finite fault simulations (Edwards et al. 2019) using source, path and site parameters obtained from inversion of the Fourier amplitude spectra of recorded motions in the field. While the extrapolation to the largest magnitudes currently considered in the hazard and risk calculations (see Bommer and van Elk 2017) is inevitably associated with large epistemic uncertainty, the model is well calibrated to local conditions by virtue of the database of recorded motions from the field. The site response model (Rodriguez-Marek et al. 2017) is also calibrated to the field conditions through the development of a detailed shear-wave velocity

model from the surface to the reference rock horizon over the entire field (Kruiver et al. 2017). The site response model and GMM have also served as key inputs into the development of a Groningen-specific liquefaction hazard assessment (Green et al. 2019).

An overview of the historical development of the permanent Groningen recording networks is provided by Dost et al. (2017). The purpose of this paper is to present some more details about the characteristics of the networks and the instruments with a view to providing insight into the usability of the growing number of recordings, which form an exceptional database of ground motions from induced earthquakes. Such an evaluation is of interest also because it is a rather unique situation to have so many networks operating simultaneously in a relatively small region. Indeed, the comparison of recordings from the different networks highlighted a configuration error in one of the networks, which has consequently been resolved. Another interesting feature of the Groningen field is a network of accelerographs installed in private houses, and often not at ground level but rather on the lower portions of walls, a situation that may be analogous to networks being installed within smart electricity meters in other parts of the world (e.g. Abrahamson et al. 2017). The paper describes an extensive programme of investigation, using field and laboratory experiments, to ascertain to what degree the recordings from these instruments can be used in practice to characterise the ground-motion.

Following this brief introduction, Sect. 2 provides an overview of the Groningen networks, including their installation, instrument characteristics and usable frequency bands. Section 3 discusses comparisons of the recordings from the different networks and the degree of consistency displayed. Within that discussion, we explain how the configuration error was identified and resolved, including a brief assessment of the impact of the error on the ground-motion modelling endeavours. Section 4 then describes the work undertaken to explore the usability of the wall-mounted accelerograph recordings in the Household network, before concluding with a brief discussion in Sect. 5.

2 Recording networks in the Groningen field

2.1 Overview

The Royal Netherlands Meteorological Institute (KNMI) had already been operating a small accelerograph array since 1997 when the M_L 3.6 Huizinge earthquake occurred in 16 August 2012 (Dost et al. 2017). Following this event, the existing network was upgraded and expanded to form what is now known as the B-network. Additionally, NAM funded the installation of three more ground-motion recording networks in the region of Groningen between 2014 and 2017: (a) the G-network, an array of 79 stations, including 69 borehole stations, also operated by KNMI; (b) the Household network, consisting of more than 300 accelerographs located in private residences and public buildings, operated by research organisation TNO; and (c) accelerographs placed in local NAM facilities as part of a traffic lights system, which are operated by NAM. The locations of the stations of these networks are shown in Fig. 1. A fifth network has operated periodically in the field since 2016, known as the 'flexible network', and consists of redeployable geophones which have been temporarily installed in different locations.

The different stages of installation and operation of the networks are presented in Fig. 2, while the basic information of the different networks, as well as the characteristics of their sensors, are presented in Table 1. As can be seen, the upgrade of the B-network and the installation of the new accelerograph networks began within 2 years of the Huizinge earthquake.

2.2 The B-network

The B-network is the standard accelerograph network of the Groningen field and has been operated by the KNMI. Since the installation of its first station in 1997, its size gradually increased until 2009, when the network comprised of 12 stations. Following its expansion, which took place in 2013–2014, it reached a size of 17 stations, two of which have been discontinued since, making the current number of stations 15. All but two of the stations are located in the north of the field, where most of the seismicity has occurred
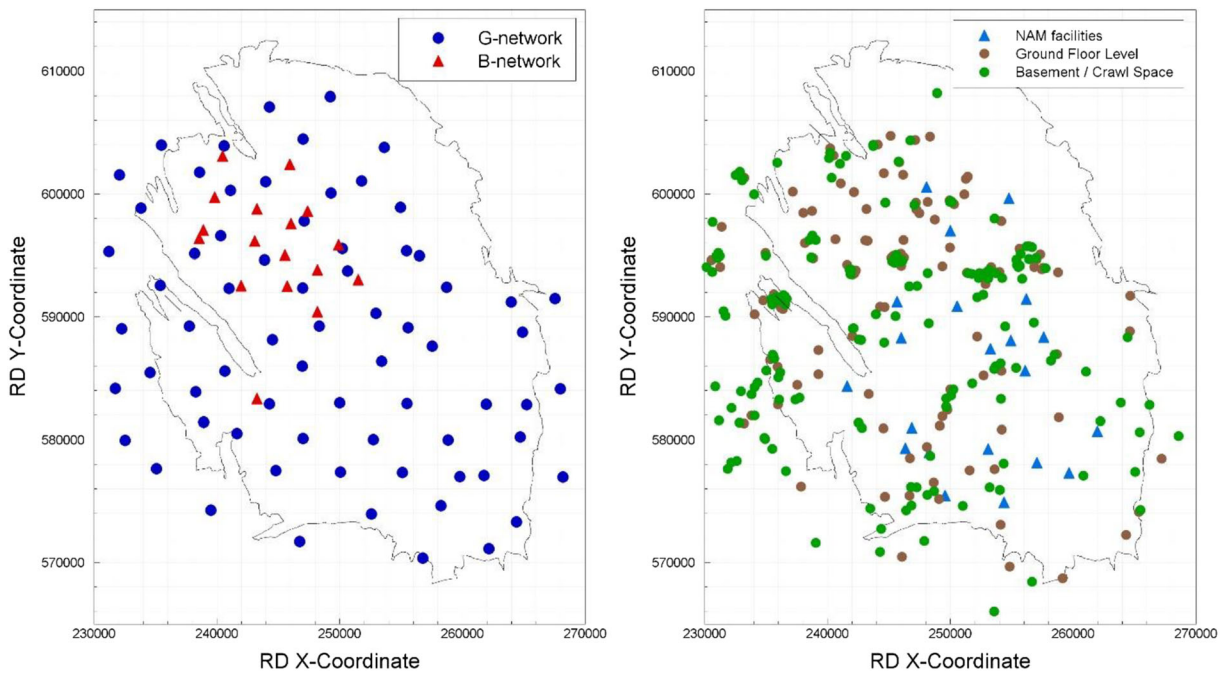
Fig. 1 Station locations of the KNMI B- and G-networks (left) and the NAM facilities and Household networks (right) in and around the Groningen field (outline in black)

by virtue of being in the centre of the compaction. The B-network was the only network operating at the time of the Huizinge earthquake in 2012 and early GMM development work relied exclusively on recordings from this network. To enhance the usefulness of the B-network recordings, a series of in situ shear-wave velocity (V_S) measurements were conducted in close proximity to these stations (Noorlandt et al. 2018). These

measured V_S profiles were found to be in good agreement with the profiles constructed from the shallow geological model for the region as presented by Kruiver et al. (2017).

The B-stations are equipped with EpiSensor ES-T accelerographs, connected to 24-bit Kinemetrics dataloggers. The EpiSensor accelerographs have a ± 4, ± 2, ± 1, ± 0.5 or ± 0.25g range, while the Obsidian dataloggers have a 127-dB dynamic
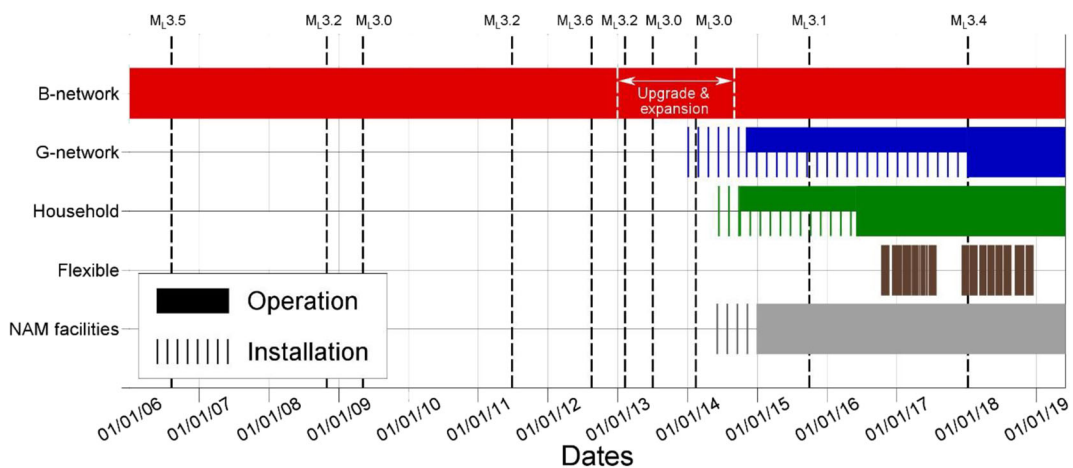

Fig. 2 Stages of installation and operation of the ground-motion recording networks in the Groningen field. The occurrence of earthquakes of local magnitude equal or greater than 3.0 is also denoted in *black dashed lines*

Table 1 Main characteristics of the ground-motion networks in the Groningen field currently

| Network	No. of stations	Sensor type	Model	Sensor location	Sample rate (Hz)	Operator
B	15	Accelerograph	EpiSensor FBA ES-T	Ground-floor of buildings	200	KNMI
G Surface (G0)	79	Accelerograph	EpiSensor FBA ES-T	Remote locations	200	KNMI
Borehole (G1–4)	69	Three-component geophone	ION Sensor SM-6H	One at every 50 m-depth down to 200 m	200	KNMI
Household	~ 300	Accelerograph	GeoSig AC-73	House walls	250	TNO
Flexible	400–450	Three-component geophone	GEOSPACE GS-ONE-LF	Surface (30 cm depth)	250	Rossingh Geophysics
NAM facilities	66	Accelerograph	GeoSig AC-73	Ground-floor	250	NAM

range, defining the smallest possible increment in motion that can be represented, between clip levels and typical self-noise. Recording at a sampling rate of 200 Hz, the Obsidian provides a flat frequency response between DC (0 Hz) and 80 Hz, after which a strong anti-alias filter diminishes the signal amplitude to avoid signal aliasing. Earthquake ground motions at the surface generally contain energy well below this limit.

Prior to the B-network upgrade, the stations consisted of GeoSig AC-23 (geophone-based force-feedback) or AC-63 (MEMS based) accelerographs with ± 2 g on scale recording. The AC-23 were connected to GSR-16-2 16-bit dataloggers, while the AC-63 sensors were connected to GSR-18 18-bit dataloggers. The usable dynamic range of the GeoSig dataloggers is 108 dB at 200 Hz. This implies that the resolution is about an order of magnitude less than the newer instruments (Fig. 3), but still very good for ground-motion recording.

In order to acquire accurate values of PGV and long-period response spectral accelerations, it is necessary to apply a low-frequency (high-pass) filter to the records. This was done by applying an 8th order acausal Butterworth filter. A filter of a different corner frequency was applied to each record, which was determined by an iterative process. First, the frequency at which the decay of Fourier spectra of the record towards low frequencies deviates from the f^2 curve is selected. The record is then filtered, and the displacement trace computed. If the final displacement is zero and long-period noise is not discernible in the displacement time-series, then no further filtering is required. Otherwise, a higher frequency is selected, and the process is repeated until these criteria are met. The same filter is applied on both horizontal components of each recording to retain compatibility of their timings, while the acausal nature of the filter ensures that there is no phase distortion of the record.

Akkar and Bommer (2006) present two theoretical models for the corner frequencies of low-cut filters, the JB88 model, resulting from Brune's single-corner source spectrum model for a stress parameter of 100 bar, and the AS00 model, computed from the double-corner source spectrum, which has upper and lower bounds T_a and T_b. These models were derived for records of earthquakes of larger magnitudes; in Fig. 4, however,

Fig. 3 Example recordings at station WIN and BWIN (upgraded WIN, post-2013) highlighting the 80-Hz anti-alias filter. Top left: WIN record of the M_L 3.0 Zeerijp earthquake (8 May 2009); top right: BWIN record of the M_L 3.4 Zeerijp earthquake (8 January 2018). Bottom: Fourier amplitude spectra of noise (i.e. FAS of data to left of vertical black line in time-series plots)
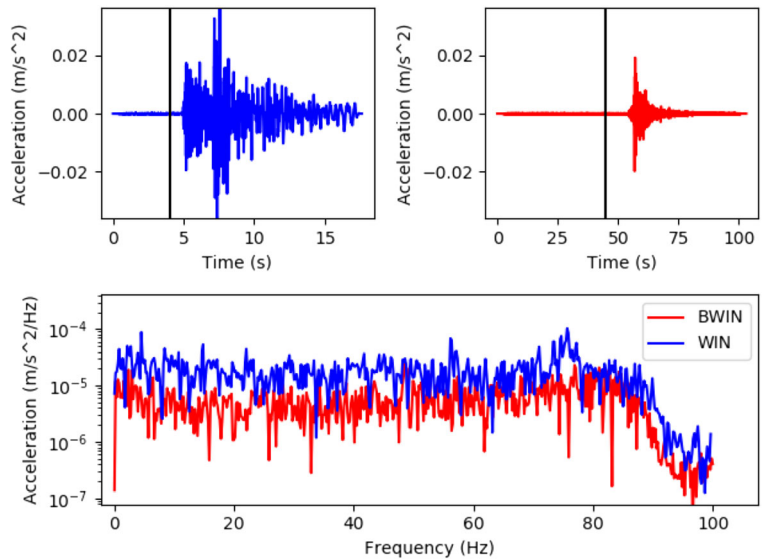
they are extrapolated to lower magnitudes and compared with the long-period cut-offs determined for the B-station records using the process described in the previous paragraph. It can be appreciated from the comparison that the cut-off periods are significantly longer than the extrapolated models would predict. Hence, the records produced by the network display remarkably high signal-to-noise ratios given their low amplitudes.

At the same time, the application of a high-frequency (high-cut) filter to the records is not necessary, as high-frequency spectral acceleration values can be accurately obtained also without removing the high-frequency noise, as they are less sensitive to the filter cut-off than long-period
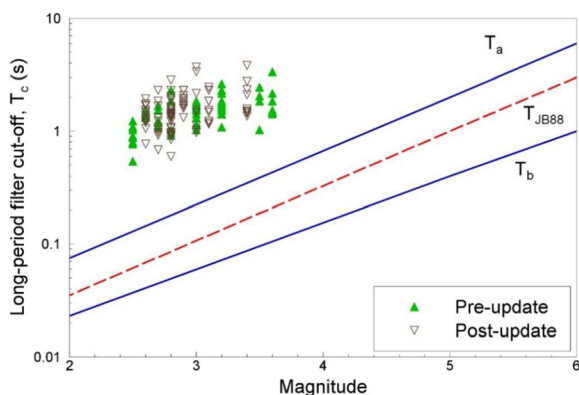

Fig. 4 Extrapolation to lower magnitudes of the theoretical cut-off period curves presented in Fig. 2 of Akkar and Bommer (2006), and comparison with the cut-offs of B-records

ordinates. This can be understood as a result of the relation between Fourier amplitude and response spectra, and the fact that high-frequency response spectral ordinates are poorly correlated with high-frequency Fourier spectra amplitudes (Bora et al. 2016). Different studies (e.g., Akkar et al. 2011; Douglas and Boore 2010) have in fact demonstrated that high-cut filters are required only in particular circumstances and are only desirable for records obtained from the older, analogue sensors, which have undergone digitisation (Boore and Bommer 2005).

It must be noted that for applications making direct use of the Fourier spectra of the records, such as the inversions discussed by Bommer et al. (2017b) and Edwards et al. (2019), the usable frequency range of the records can be defined very differently. The window of usable frequencies in this case is selected such that there is a minimum signal-to-noise amplitude ratio of 3 in all frequencies within the window. In this context, both low- and high-frequency usability limits are applied.

Records from one station, FRB2/BFB2, however, not been used due to the proximity of the station to a NAM facility, the operations of heavy machinery at which created monochromatic noise. The noise observed in the records of the station before the 2013 upgrade (Fig. 5) persists in the records obtained after the upgrade as well, confirming that the source is external.

Fig. 5 Accelerograms obtained by station FRB2 during M_L3.6 Huizinge earthquake of 16 August 2012
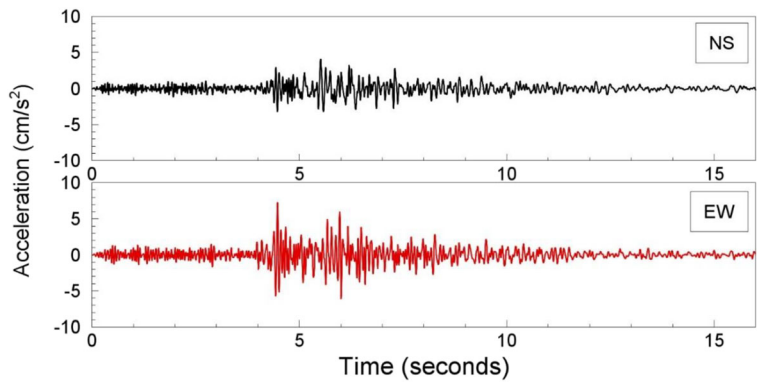
2.3 The G-network: surface accelerographs

As part of NAM's data acquisition plan, a second network was installed consisting of instrumented boreholes, each co-located with a surface accelerograph. The borehole instruments are discussed in Sect. 2.7.

The G-network currently consists of 79 surface accelerograph stations. The accelerographs are of the same model as the B-network and have the same usable frequency range. Kinematics dataloggers of the same dynamic range are also used. An example of a G-station is shown in Fig. 6.

The first G-records became available during the M_L 2.9 Wirdum earthquake of 5 November 2014 and have generated hundreds of records since then despite the reduction in seismicity levels as a consequence of

several incremental reductions in the production levels. These accelerographs (the G0 stations) were recently found to have been installed with a configuration error, as discussed below in Sect. 3.

Although no in situ V_S measurements have been performed for the G-stations, interval velocities calculated from the borehole instruments (Hofman et al. 2017) have been found to be consistent with the velocity profiles constructed by Kruiver et al. (2017) for the entire field from geological data (Noorlandt et al. 2018).

2.4 The Household network

The Household network is an array of more than 300 GeoSig AC-73 accelerographs installed between 2014 and 2016. Most of these are located inside private

Fig. 6 Exterior (left) and interior (right) of a G-station. The stations were installed in remote locations to minimize the noise recorded

residences, with a few being in the premises of public institutions and other organisations. The owners of the houses volunteered to have a sensor in their house through an online platform and have access to its live recording stream. The network is currently operated by TNO on behalf of NAM.

The installation of the accelerographs is unusual; instead of being secured on a concrete slab on the ground-floor of the houses (as the B-station accelerographs are), they are placed on metallic brackets mounted on the house walls. They are found on the wall of either the ground-floor level, the basement, or the crawl space under the ground-floor (Fig. 7).

Records from ground-floor level sensors have so far been treated with caution, as they may be contaminated by structural response through the deformation of the walls on which they are placed. Three exercises have been carried out to explore their usability; these exercises and their results are discussed in Sect. 4. Records from sensors of the

basement and the crawl space are considered usable and have so far been used in the development of the spatial correlation model of Stafford et al. (2019), given the dense spacing of the instruments over the field (Fig. 1).

The default setting of the GeoSig stations is to produce a recording only once a PGV value of 0.1 cm/s has been surpassed in any component. While this is a low value for strong-motion records of large earthquakes, it is high for the small-magnitude seismicity of Groningen. Hence, until a system to bypass the PGV threshold was set up by TNO at the request of NAM in 2016, the datasets generated during local earthquakes were censored. Only records from distances up to about 7 km, as well as the highest amplitude recordings from slightly larger distances, were obtained until then. At the same time, the sensors have been set up to transmit to the server the PGA and PGV values of each of their three components for every minute of the hour, the so-called "heartbeat data".

Fig. 7 Sensors installed on the walls at the: basement level (top left), crawl space (top right) and ground-floor level (bottom). Most sensors are located in the interior of the houses (bottom left), while some can be found in the exterior (bottom right)

2.5 The flexible network

The flexible network is an array consisting of a total of 450 portable geophones, managed on behalf of NAM by Rossingh Geophysics. It has been used for passive monitoring since October 2016 and is re-installed at a different location in the field where it remains operational for a maximum of 45 days each time (in some cases significantly less). The usability of geophone records is discussed by Campman et al. (2016), who conclude that such arrays have a wide usable frequency range.

Recordings from the flexible network have been used by NAM to infer the sub-surface shear-wave velocity profiles of different parts of the field down to 30, 100 and 800 m of depth, deployed with a mean inter-station spacing ranging up to 4 km. Studies making use of flexible network recordings include Spica et al. (2018) and Stafford et al. (2019).

2.6 The NAM facilities network

In 2014, NAM created a traffic lights system in 22 of its facilities located in the Groningen field. The creation of the traffic lights system included the installation of three accelerographs in each facility, resulting in a total number of 66 accelerographs (of the same type and setup as those of the Household network but operated separately). The purpose of the accelerographs is to trigger a safe shutdown of the facilities if a certain threshold of motion is surpassed.

This accelerograph network has generated hundreds of records since 2014; however, expectations for their potential use are low, as they will also be contaminated by monochromatic high-frequency noise emanating from the heavy machinery of the facilities, as station FRB2/BFB2 has been shown to be (Fig. 3). To date, no attempt has been made to incorporate these records into the database used to develop ground-motion models.

2.7 Borehole instruments

The levels of ambient noise recorded by the surface accelerograph stations render the detection of local events of magnitudes below $M_L 1.5$

very difficult (Dost et al. 2017). Consequently, KNMI installed a network of borehole stations each containing an array of geophones and one surface accelerograph . The first borehole station was constructed in 1991, and a total of ten had been constructed by 2010 in the wider area surrounding Groningen. After the Huizinge earthquake, KNMI installed an additional 69 borehole stations as part of the G-network. These contained four geophones, one at every 50 m down to 200 m depth. Records from all four geophones of the stations and their surface accelerograph (discussed in Sect. 2.3) have been used in work related to the site properties of the locations of the G-stations, such as the study of Spica et al. (2017).

A separate array consisting of four stations with broadband seismographs placed at 100 m depth has also recently been installed in the field. For reasons of space, however, the recordings from the borehole sensors are not considered in the remainder of the paper, which focuses exclusively on surface instruments (as indicated in the title).

3 Consistency of surface recordings

Figure 8 shows geometric mean values of peak ground velocity (PGV) obtained during the 30 September 2015 M_L 3.1 Hellum earthquake from three main accelerograph networks. Several interesting observations can be made on this plot, the first being the large loss of potentially useful data from the household network as a result of the triggering threshold.

The second observation that can be made is that the recorded PGV values seem to be broadly consistent with no obvious deviations for any of the networks. However, a similar figure presented in Bommer et al. (2017a) showed a somewhat different pattern. More specifically, the data points corresponding to the G-network had values approximately half of those shown in Fig. 8. The source of this difference is a configuration error in the surface accelerographs of the G-network, which was discovered in late 2018 and affected the scale of the records.

Fig. 8 PGV values obtained during the $M_L 3.1$ Hellum earthquake of 30 September 2015. Values for non-triggered sensors come from the "heartbeat" data—PGA and PGV values saved at the network server for each minute of the hour
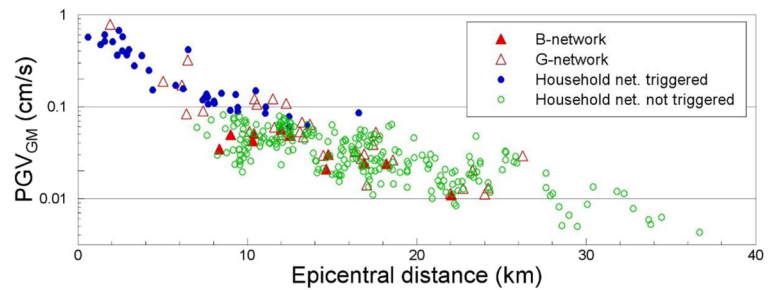
In November 2017, a set of empirical PGV ground-motion prediction equations (GMPEs) was developed for the Groningen field. The reason for this is that PGV is the basis of official Dutch guidelines for assessing the impact of vibration on buildings, as presented in the document Building Damage: Measurement and Assessment (SBR 2002). Consequently, NAM has requested Groningen-specific GMPEs for PGV to estimate the value of this parameter at specific locations due to induced events in the field. Equations were derived for three different definitions of the horizontal component of motion based on different treatments of the horizontal components from each accelerogram: the geometric mean (PGV_{GM}), the larger of the two (PGV_{Larger}), and the peak corresponding to the maximum value obtained by rotating the recorded components (PGV_{MaxRot}).

The database used in the development of this model included more than 1000 records, from many recent events of a local magnitude range of $M_L 1.8–3.6$, more than half of which originated from the surface accelerographs of the G-network. A pattern was then observed in the model residuals that indicated an apparent decreasing trend in the average motions after the end of 2014. One possible explanation for this observation was that stress drops in the seismicity of the field were decreasing, which could, for example, be the result of faults being re-activated multiple times. Another explanation, however, was that since this decrease in average motions coincided with the installation and start of operation of the G-network, the G-network was producing systematically lower-amplitude recordings. This line of thought was reinforced when the $M_L 3.4$ Zeerijp occurred in 8 January 2018 and, despite the fact that it generated the largest-amplitude recording of the Groningen database, the average motions from this event were also relatively low.

The investigation began with a comparison of records obtained during recent earthquakes from closely located B- and G-stations. One such example is shown in Fig. 9, where the amplitude of the B-station recording is clearly seen to be larger than that of the G-station. The difference observed in the right frames of Fig. 9 was consistent in recordings generated during different events and in other closely located B- and G-stations.

This prompted further investigations comparing waveforms from all stations but not using recordings from local seismicity, because of the large amplitude variations from station to station due to radiation effects, complex propagation effects and varying site amplification effects. Using regional or teleseismic arrivals, the amplitude variations are less complex. For distant sources, the stations in Groningen experience practically the same source radiation and a single phase can be selected that is consistently recorded over all stations. Hence, recordings obtained from very distant tectonic events were used for the comparisons (Fig. 10). Records from an existing (NARS; Yudistra et al. 2017) and the newly installed broadband seismograph array were also used in these investigations.

Figure 10a shows the recording of a PKIKP phase over Groningen from a large earthquake in Fiji. This is a P-wave phase that traverses the Earth's outer core before traveling through the mantle and crust at the receiver side. Due to its steep angle of incidence, most energy of this longitudinal wave resides on the vertical component (the red traces in the figure) but much of the subsequent coda is also recorded on the horizontal components (blue and green traces in the figure). The waveforms have been band-pass filtered between 0.4 and 0.9 Hz.
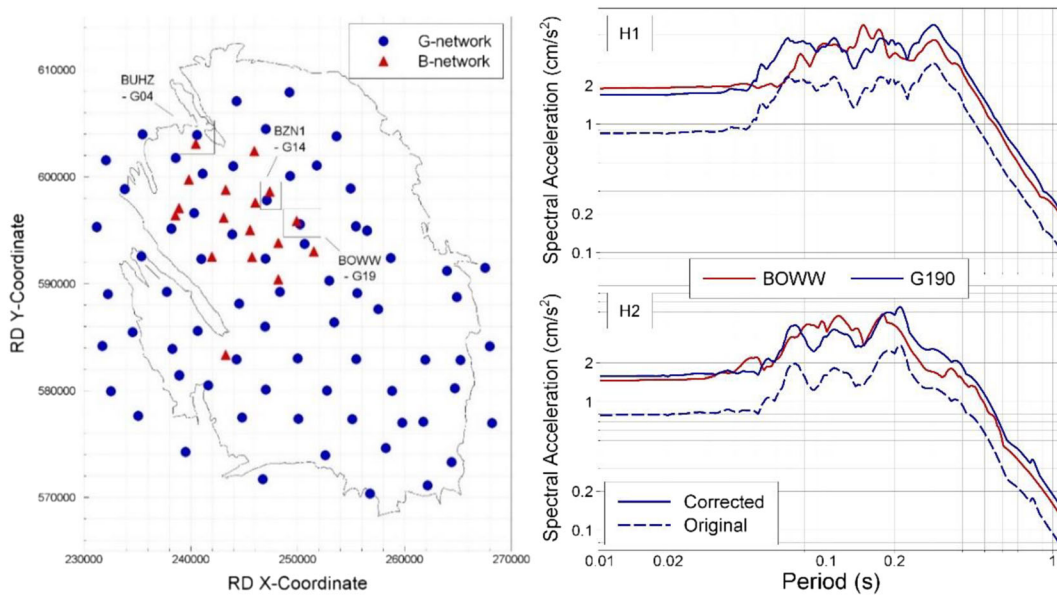
Fig. 9 Left: Map showing pairs of closely located B- and G-stations; right: pseudo-acceleration response spectra of records obtained at a pair of collocated stations during the 30 September 2015 M_L3.1 Hellum earthquake; the spectra of the G-station are shown before and after the correction

Figure 10b shows the maximum amplitudes expressed in particle velocity. These are the maximum absolute values as obtained from the vertical component and the time window and frequency band shown in Fig. 10a. Both panels in Fig. 10 have the same ordering of stations. Due to the large depth (558 km) and large magnitude (8.2) of the Fiji earthquake, the PKIKP arrival has high signal-to-noise ratio and is recorded with significant amplitudes in Groningen (up to about 0.6 mm/s).

Figure 10 shows a systematic maximum amplitude difference between the different networks, confirming that the records of the G-network accelerographs had different scales. More specifically, the G010-G700 records had, on average, only half the amplitudes of the B-network, while the G710-G800 records had twice those amplitudes. The amplitudes of the broadband stations are close to the ones recorded by the B-network.

The cause of the error was finally identified after examination of accelerographs from different stations in the labs of the KNMI. Accelerographs record counts of change in the voltage of the transducers due to acceleration. The proportion of volt counts to acceleration (in m/s^2) is called the instrument gain and is used to translate the recorded volt counts back to acceleration. Despite the fact that the B-network and G-network accelerographs are of the same model, they have a small difference in their circuit jumpers which affects the

voltage of the transducers. Hence, a different configuration is required for the gain of G-network and B-network accelerographs to be the same. Because the accelerographs are of the same model, this was not detected, and the G-stations were set up with the same settings as the B-stations. Thus, the real gain of stations G010-G700 ended up being half the gain of the B-stations, while the gain of G710-G800 was double. However, the gain used to translate the volt counts to acceleration was that of the B-stations, resulting in the error in the scale of the records.

In early December 2018, the KNMI corrected the instrument response inventories to reflect the real gain the stations have. Using the correct gain to translate the volt counts to accelerations eliminates the scaling error. By that time, records from the G0 stations had been included in the databases used for some applications. The impact of the error on the development of the ground-motion models for the prediction of peak ground motions, spectral accelerations and durations that are used in the hazard and risk modelling is discussed in Dost et al. (2019), an erratum to Dost et al. (2018). The conclusion of the review by Dost et al. (2019) was that the ground-motion models on which NAM and KNMI hazard modelling is based were entirely (and fortuitously) unaffected by the error. A key factor in this conclusion is that when the model-building began to

Fig. 10 Recording of a PKIKP phase over Groningen due to an earthquake in Fiji; **a** the 3-component filtered waveforms and **b** the maximum amplitudes on the vertical component. Data from the B-stations are shown in red, the G010-G700 stations in blue full triangles, the G710-G800 stations in open triangles and the broadband stations in green full triangles
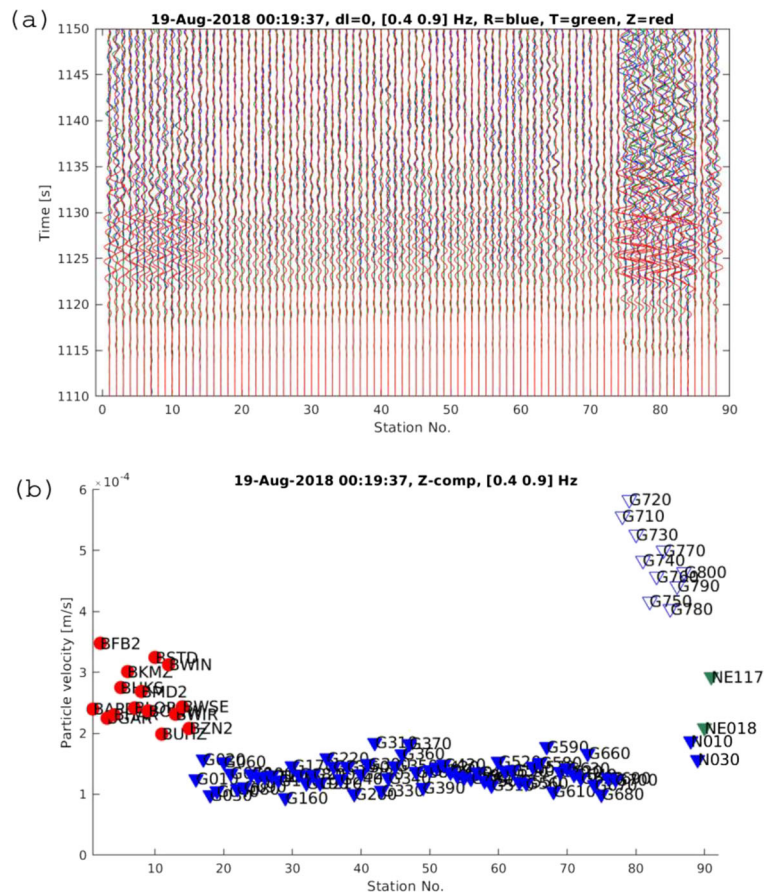
incorporate G-network recordings, the 200-m borehole geophone recordings were adopted rather than the surface accelerograms, for reasons explained in Bommer et al. (2017b).

The only impact of the G0 configuration error was on the derivation of the empirical GMPEs for PGV. The models predicting median PGV values do change as a result of the correction, leading to modest increases in predicted PGV values for smaller magnitudes and particularly at longer distances. However, at M_L 4.0, which is slightly above the strict limits of applicability, the correction leads to a small reduction in predicted PGV values at short distances. This can be observed in Fig. 11, which compares median predicted PGV values from the original and corrected models as a function of distance for three different magnitudes and as a function of magnitude for different distances.

Additionally, there was a large change in the inter-event variability, which was reduced by approximately a factor of two, and consequently a change to the total variability (sigma) of the model; previously, the inter-event variability was inflated by erroneous large negative event terms associated with the recent earthquakes dominated by recordings from the G0 stations compared to the earlier earthquakes, including Huizinge, which were exclusively recorded by the B-network stations.

With the scale of the G-network records corrected, a question that arises is whether there are differences in the recordings resulting from the differences between the free-field installation of the G accelerographs and the within-building installation of the B-stations. This is difficult to determine only by comparing from pairs of closely located instruments since most of the pairs of stations are close to 1 km or more apart; the only pair of stations that is relatively close (BOWW-G190, which are 430 m apart) yield very similar recordings (see Fig. 9). Well-recorded earthquakes do suggest that there might be a tendency to record lower short-period amplitudes at the B-stations but this is only the case for weaker motions recorded at greater distances (Fig. 12). Such a trend, if consistent, might be related to the effects of the buildings or their foundations, and a consequence
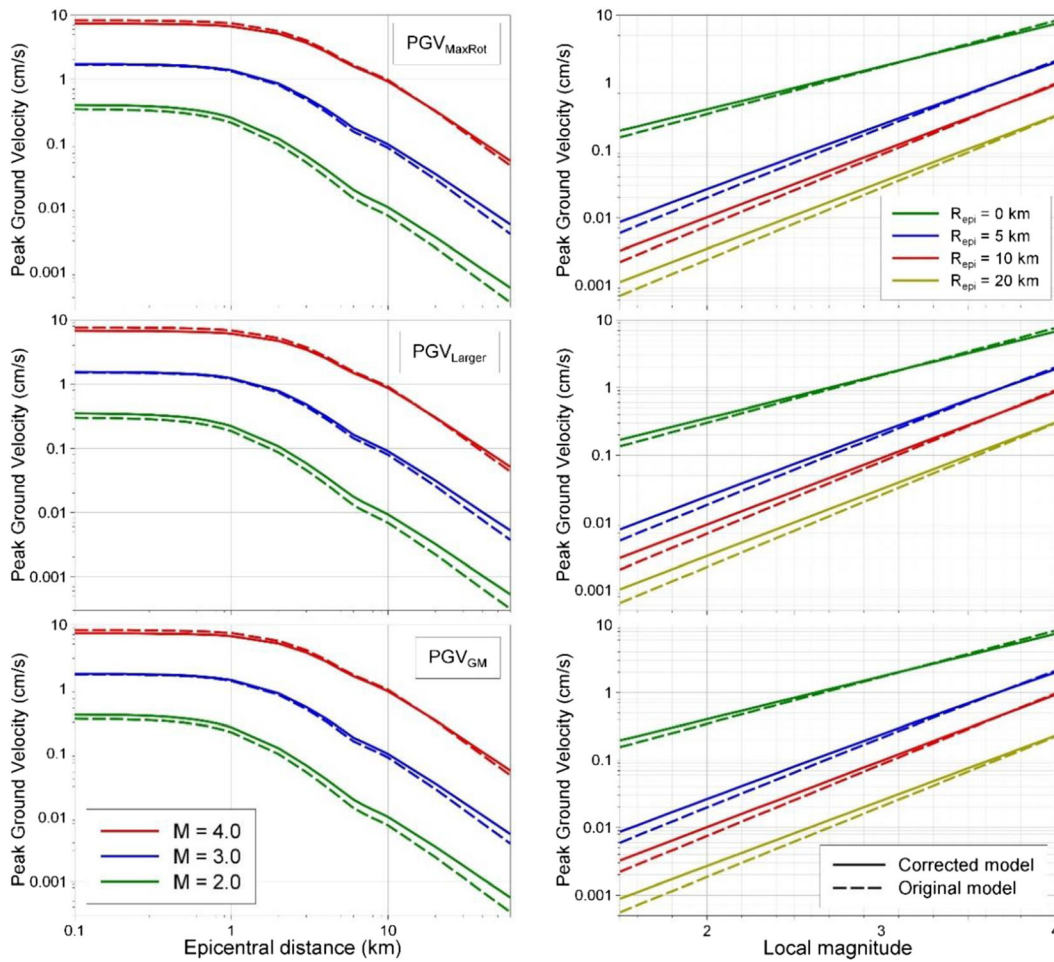
Fig. 11 Predicted median PGV values from the original and corrected models against distance for magnitudes M_L 2, 3 and 4 (left) and against magnitude at four different values of epicentral distance (right)

of the very soft soil conditions in the field (where average V_{S30} values are on the order of 200 m/s). The B-stations have recorded the largest amplitudes of motion to date and we would not consider it appropriate to exclude them from the database used for ground-motion modelling.

4 Usability of records obtained from wall-mounted Household network sensors

The TNO-operated household network is potentially a very rich source of data, given the large number of stations and their distribution over the field. However, as has been highlighted in the preceding sections, the usefulness of the data obtained from this network is potentially limited by the triggering mechanism that has been imposed (Sect. 3)

and by the unconventional installation of many of the instruments (Sect. 2.4). Two separate lines of investigation were initiated to explore the usability of recordings from the unusually installed instruments mounted on brackets at some height on the wall.

4.1 Installation of additional sensors on houses of the Household network

The first experiment was field-based and dependent on the occurrence of new earthquakes: it was decided that two more accelerographs would be installed in a sample of houses of the network, one on the floor directly under or next to the existing sensor, and another one on a concrete slab in the garden (replicating free-field conditions as much as possible). A sample of 25 houses was selected such that (a) all necessary information about the
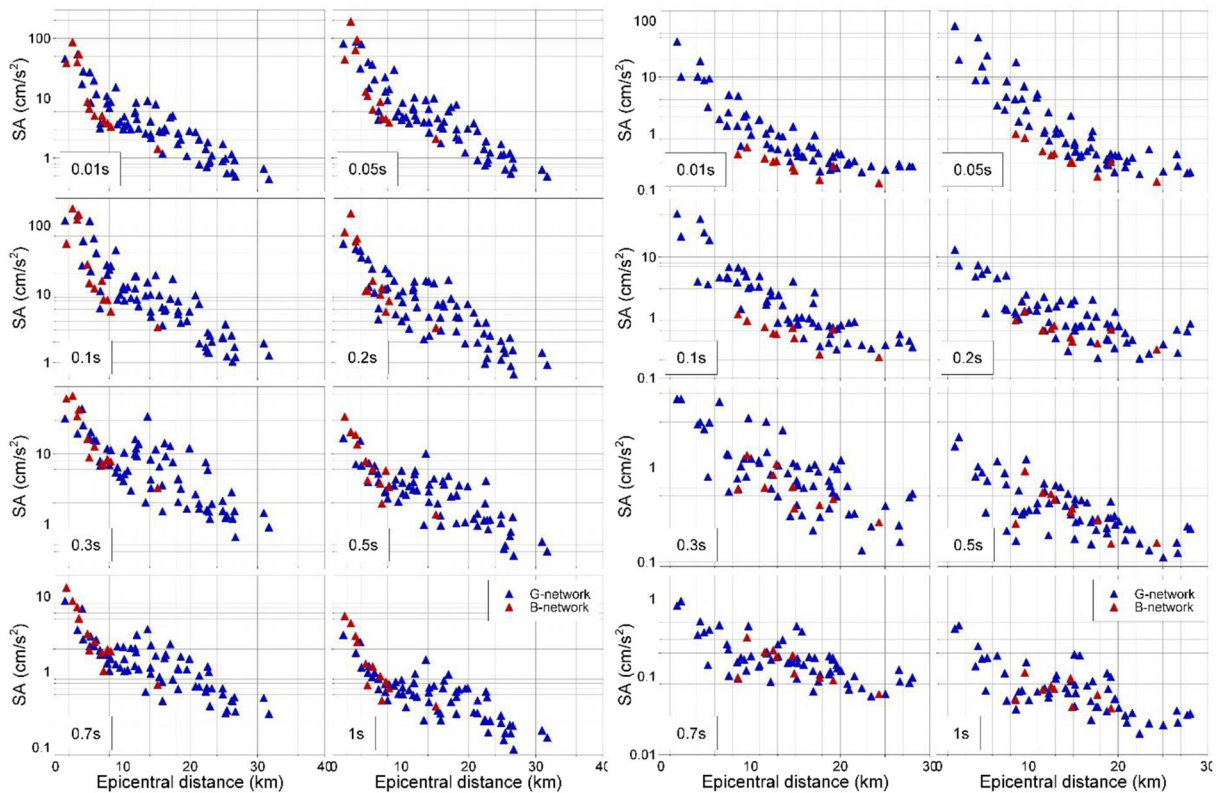
Fig. 12 Spectral accelerations at different periods against distance from the January 2018 M_L 3.4 Zeerijp earthquake (left) and from the May 2017 M_L 2.6 Slochteren event (right)

houses and the stations is known and the stations are accessible, (b) the typologies of the selected buildings are representative of all buildings of the network and (c) the houses are in the north of the field, where seismicity is more frequent and hence they will be able to record a clearer signal.

Residents were hesitant to install more accelerographs and especially to add concrete slabs to their gardens; thus, the exercise was delayed. In 2016, the geophones of the flexible network became available, and it was decided to use some of those instead of accelerographs. Most residents agreed to a geophone installation, which is temporary and much less invasive, while some others even volunteered to have one installed in their house. Geophones were finally installed in 16 houses between April and September of 2017 by the operator of the flexible network, Rossingh Geophysics. Two examples are shown in Fig. 13.

The installation of geophones from the flexible network, while convenient and acceptable by the residents, resulted in a number of limitations and differences . The first of those is that the records to be compared were obtained by two different types of sensors. Secondly, a notable difference of the installation of the geophones to the layout originally planned was that the geophone that was placed in the garden was not placed on a concrete slab (a feature which was also considered undesirable by the residents) and was buried 30 cm deep. At the same time, due to differences between the accelerographs and the geophones in the size and the layout of the bolting connections, the geophones could not be installed on the same metallic brackets on which the accelerographs were. Instead, a different type of metallic bracket, smaller and significantly lighter, was constructed by Rossingh Geophysics.

In some houses, the geophones were not installed next to the accelerographs, due to limitations of space and due to the preferences of the residents, which were also taken into account. In most cases, the geophones of the garden were also not placed close to the location of the accelerograph, but in locations that were also considered more convenient for the needs of the installation process.

Fig. 13 Examples of geophones installed next to existing Household network accelerographs. The accelerograph in the right frame is inside the silver cover

On 8 January 2018, a M_L3.4 earthquake occurred in Zeerijp, in the North of the field. The geophones had been pre-set to record a maximum recording amplitude corresponding to about 0.35 cm/s; hence, geophones in ten houses with small epicentral distances clipped and did not produce usable records; usable records were produced in only six of the houses. The pseudo-acceleration response spectra, Fourier amplitude spectra and velocity traces recorded in one of the houses are presented in Figs. 14 and 15. The epicentral distance of that house was 4.97 km. The FAS shown in Fig. 15 have been smothed using the procedure provided by Konno and Ohmachi (1998).
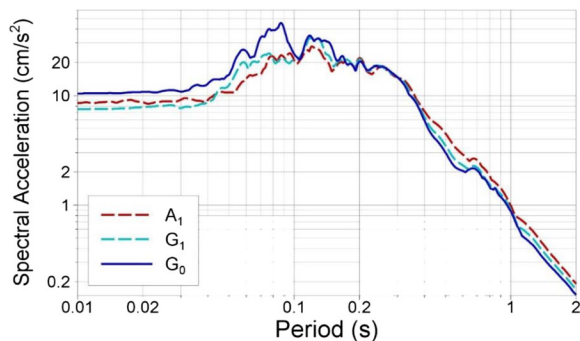
4.2 Installation of sensors on shake table test houses

The second approach was laboratory-based and designed to take advantage of experimental work being conducted to quantify the seismic fragility of typical houses in the Groningen field (Graziotti et al. 2018). A major benefit of this approach was that it did not depend on earthquakes in the field. Two tests of full-scale structural specimens were considered; the first took place in May 2017 and regarded a terraced house configuration (LNEC-BUILD1, Tomassetti et al. 2019), while the second was carried out in March 2018 and addressed detached house typologies (LNEC-BUILD3, Kallioras et al. 2019).
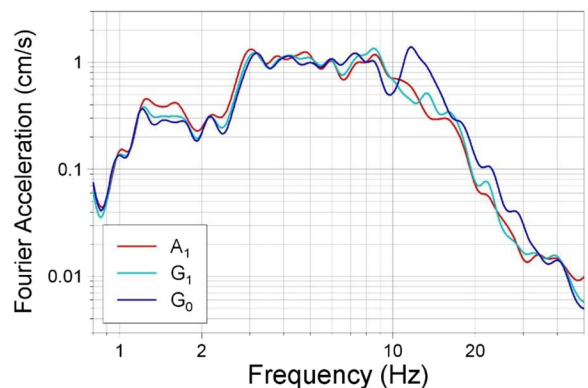

Fig. 14 Pseudo-acceleration response spectra of the H1 component of records obtained from the accelerograph and the additional geophones placed at a house of the Household network, during the 8 January 2018 M_L3.4 Zeerijp earthquake. A/G denotes the sensor type (A: accelerograph, G: geophone) while the subscript denotes the level on the wall

Fig. 15 Fourier amplitude spectra of the H1 component of records obtained from the accelerograph and the additional geophones placed at a house of the Household network, during the 8 January 2018 M_L3.4 Zeerijp earthquake. A/G denotes the sensor type (A: accelerograph, G: geophone) while the subscript denotes the level on the wall

In the first exercise, a total of eight sensors were installed. One accelerograph, identical to those of the Household network, and one flexible network geophone next to it, were installed in each of four locations: on the north wall, at a height of 45 cm, on the test house base directly below that point, on the east wall at the same height, and on the base in front of the east wall. Sensors were installed in two perpendicular walls because the house was loaded uniaxially and the walls would respond differently, with one deforming in-plane and the other out-of-plane. The east wall was a single-wythe wall made of white calcium-silicate bricks while the north wall was a double-wythe cavity wall with an inner leaf equal to the east wall and an outer leaf made of perforated clay bricks. The test house and the sensors can be seen in Fig. 16. Response spectra and Fourier amplitude spectra recorded in the direction of uniaxial loading of the test are presented in Figs. 17 and 18.

In the second exercise, six accelerographs were installed at height intervals of 25 cm, up to 1.25 m. The recorder of the highest accelerograph did not retain the records, and therefore only records from the lower five are available (Figs. 19, 20 and 21). The motivation behind this deployment of sensors was to measure the possible variation of the influence of structural response in the lowermost 1.25 m of the wall (Fig. 19). The walls of the test house of the second exercise were thick double-wythe solid clay brick walls with the Dutch cross brickwork bond, more rigid than those of the first exercise. Comparisons of response spectra and Fourier spectra from the records obtained are shown in Figs. 20 and 21. The FAS shown in Figs. 18 and 21 have also been smothed using the procedure provided by Konno and Ohmachi (1998).

4.3 Discussion of results

The pictures that emerge from the two lines of investigation are somewhat different, although in making any comparisons, it is important to note that the amplitudes of the recorded earthquake motion in Figs. 13 and 14 are significantly lower than those

Fig. 16 The specimen house during the first shake table test at the LNEC in Lisbon (LNEC-BUILD1). Six sensors are visible: two installed at a height of 0.45 m on the eastern wall (made of white calcium-silicate bricks), two installed on the eastern wall's foundation base (detail in top right frame) and two on the northern wall's foundation base (detail in bottom right frame). The remaining pair is installed at 0.45 m on the northern internal wall, to the right of the door. The blue sensors are the accelerographs and the orange sensors are the geophones
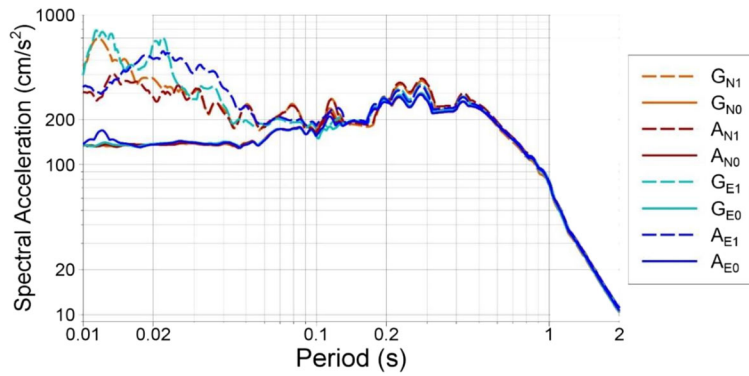
Fig. 17 Pseudo-acceleration response spectra of the H1 component of records obtained from the accelerographs and the geophones placed on the test house of the first test at LNEC in May 2017 (LNEC-BUILD1). A/G denotes the sensor type (A: accelerograph, G: geophone) while the letter in the subscript denotes the wall (East/North) and the number the level on the wall

from the shake table tests (Figs. 16, 17, 19 and 20). The shake table tests show a consistent and clear pattern: the Fourier spectra from the ground-level and wall-mounted instruments are very similar for frequencies up to about 15 Hz and the response spectral ordinates are very similar at oscillator periods greater than about 0.1 s. These results would suggest that the response spectra for periods greater than 0.1 s could be used with confidence. The PGV values, which are known to be dominated by the contributions of FAS frequencies below 15 Hz and in the Groningen database are strongly correlated with spectral accelerations at 0.3 s (Bommer et al. 2017a), are also usable, the test results showing that these values are also unaffected by the unusual

installation configurations. Conversely, short-period acceleration spectral ordinates and PGA values from these instruments are likely to be strongly distorted by the building response and therefore should not be used.

The response spectra of the records obtained in the field during the Zeerijp earthquake at a house in Groningen (Fig. 14) shows a significantly smaller difference between the response spectra of the ground-level geophone and the mounted sensors. In fact, the record from the external
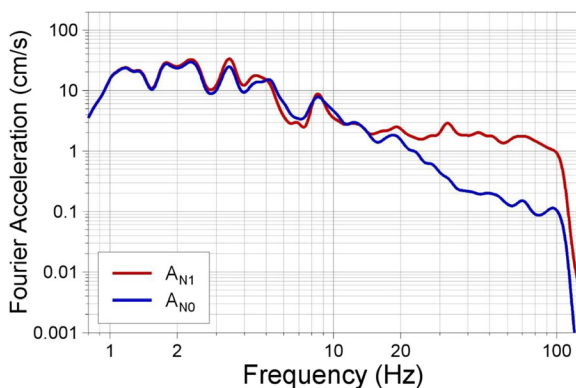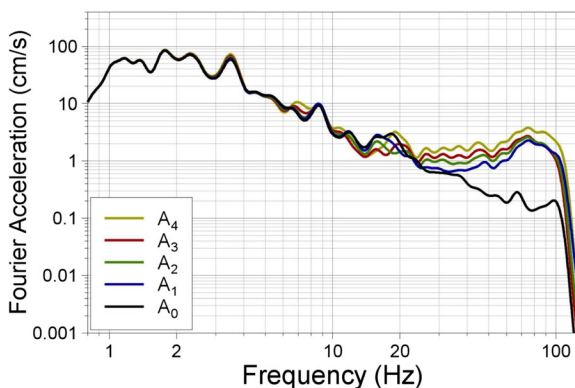

Fig. 18 Fourier amplitude spectra of the H1 component of records obtained from a pair of accelerographs placed on the test house of the first test at LNEC in May 2017 (LNEC-BUILD1). A/G denotes the sensor type (A: accelerograph, G: geophone) while the letter in the subscript denotes the wall (East/North) and the number the level on the wall

Fig. 19 Detail of the specimen house during the second shake table test at the LNEC in Lisbon (LNEC-BUILD3). Six GeoSig AC-73 accelerographs are visible: one installed on the base of the test house and five mounted on the wall at height increments of 20 cm, up to a wall height of 1.25 m

Fig. 20 Pseudo-acceleration response spectra of the H1 component of records obtained from the accelerographs and the geophones placed on the test house of the second test at LNEC in March 2018 (LNEC-BUILD3). "A" denotes the sensor type (accelerograph) while the number in the subscript denotes the level on the wall
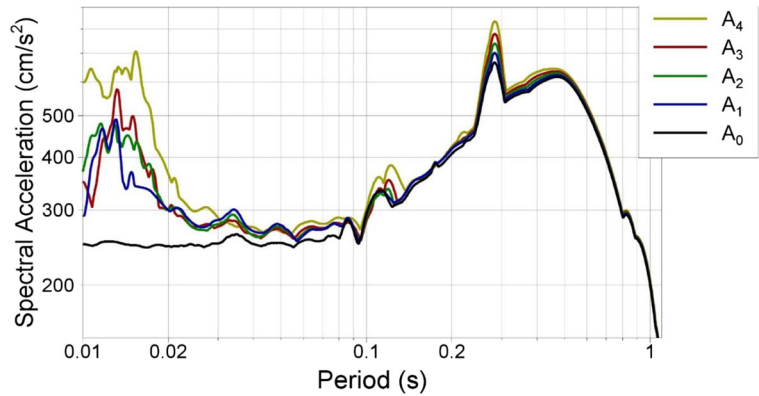
instrument yields somewhat higher spectral ordinates at short periods compared to those installed inside the house. This observation might point to a degree of suppression of the ground motion by the structure, at least at these low amplitudes of shaking. In view of possible differences between within-building and free-field motions and also the use of two different types of instruments, the field tests are viewed as being less informative and less reliable than the shake table results.

The conclusion that PGV values and spectral ordinates at intermediate periods from the wall-mounted household accelerographs could be used in ground-motion modelling exercises potentially enables a very significant expansion of the already abundant Groningen ground-motion database. The value of expanding the database of small-magnitude recordings would reside in better

Fig. 21 Fourier amplitude spectra of the H1 component of records obtained from a pair of accelerographs placed on the test house of the second test at LNEC in March 2018 (LNEC-BUILD3). "A" denotes the sensor type (accelerograph) while the number in the subscript denotes the level on the wall

constraint of spatial variability and spatial correlation, but it is important to acknowledge that it has little impact on the reduction of the large epistemic uncertainty associated with extrapolation of the ground-motion predictions to earthquakes of larger magnitude, as currently considered in the seismic hazard and risk calculations.

The tests performed in Groningen were specific to determining the usability of recordings from instruments that were installed on wall-mounted brackets. While that might appear to be a very local issue, the findings may be of relevance to applications outside of Groningen. For example, there is a scheme underway to install accelerometers within smart electricity meters in homes in southern California, which will create enormous and very dense ground-motion recording arrays (Norm Abrahamson, UC Berkeley, personal communication, 2017). However, the smart meters are usually installed at some height on the walls of houses (Fig. 22), similar to the situation encountered in many stations of the Household network in Groningen. Tests performed by installing a second accelerograph at ground level in southern California yielded very similar results to those observed in Groningen, with pronounced structural amplification of FAS at frequencies greater than 10 Hz with lower-frequency amplitudes being unaffected (Fig. 22).

5 Discussion and conclusions

The Groningen gas field in the Netherlands has become a unique full-scale laboratory for the study of induced seismicity, with exceptionally dense
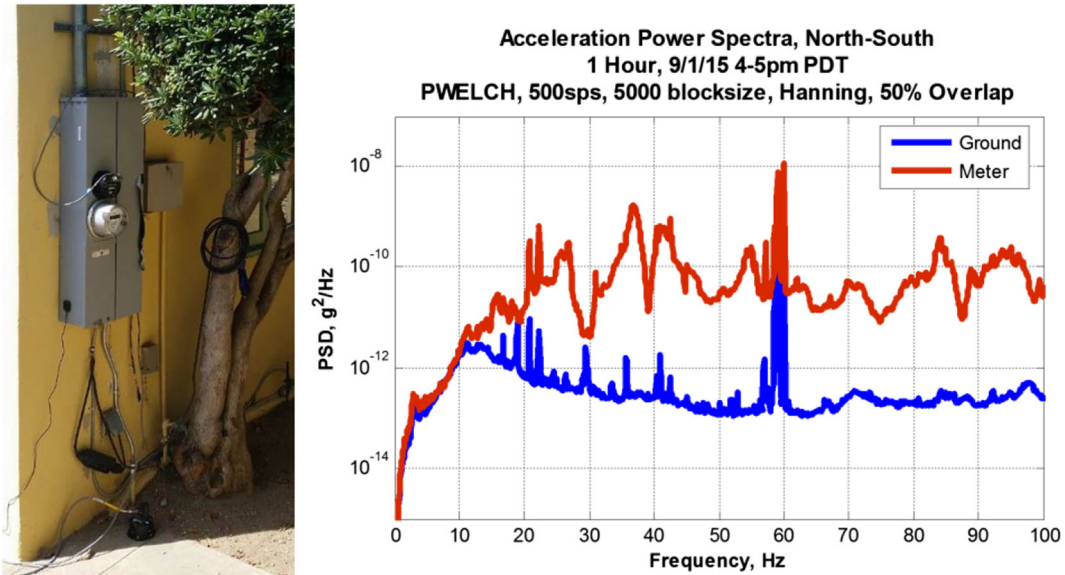
Fig. 22 Left: installation of an EpiSensor accelerograph (black) at smart meter height and on the ground below; right: comparison of the power spectral density of the sensor that is installed on the wall to the sensor that is installed on the ground underneath (images courtesy of Norm Abrahamson and Robert Nigbor)

networks of seismic recording instruments, supplemented by characterisation of the near-surface velocity profiles. Given the very specific characteristics of the field in terms of the depth and location of the reservoir, the nature of the faults being reactivated, the underlying and overlying geological units, and the soft near-surface deposits, bespoke ground-motion and hazard models are being developed that are unlikely to be directly applicable to other cases of induced seismicity, although the modelling approaches could be adapted to other locations. Moreover, the dense instrumentation in Groningen does provide a unique opportunity to characterise and model ground shaking from induced earthquakes.

In this paper, we have provided an overview of the different ground-motion networks that operate in the Groningen field. The paper has also highlighted how the installation of multiple networks facilitated the identification of a configuration error in one set of instruments; had this network been operating alone, the problem may have gone undetected.

Tests performed using additional field instruments and instrumented shake table tests on full-scale models have provided valuable insights into the usability of recordings from wall-mounted instruments on the ground level of buildings. Apart from spectral ordinates at short periods (< 0.1 s) and PGA, the finding is that most amplitude-based parameters can be used as reliable representations of the ground motion. Clearly, this finding is specific to the houses encountered in the Groningen region but it also appears consistent with data from California.

Data availability The datasets generated by the B- and G-networks analysed during the current study are publicly available in the KNMI Seismic and Acoustic Data Portal, http://rdsa.knmi.nl/dataportal/, with the exception of records from events that occurred from the older stations of the B-network, which are available upon request to KNMI. Records from the Household network (anonymised because of privacy issues), the Flexible network, and the exercises carried out in the shake table tests and in the houses in the Groningen field are available upon request to NAM.

References

Abrahamson N, Bachhuber J, Nigbor B, McCallin D, Jahanger N, Wooddell K (2017) Ultra-Dense Ground Motion Measurements and Modeling. Conference presentation, EERI Annual Meeting 2017, Portland, OR, United States

Akkar S, Bommer JJ (2006) Influence of long-period filter cut-off on elastic spectral displacements. Earthq Eng Struct Dyn 35(9):1145–1165

Akkar S, Kale Ö, Yenier E, Bommer JJ (2011) The high-frequency limit of usable response spectral ordinates from filtered analogue and digital strong-motion accelerograms. Earthq Eng Struct Dyn 40(12):1387–1401

Bommer JJ, van Elk J (2017) Comment on "The maximum possible and the maximum expected earthquake magnitude for production-induced earthquakes at the gas field in Groningen, The Netherlands" by Gert Zöller and Matthias Holschneider. Bull Seismol Soc Am 107(3):1564–1567

Bommer JJ, Dost B, Edwards B, Stafford PJ, van Elk J, Doornhof D, Ntinalexis M (2016) Developing an application-specific ground-motion model for induced seismicity. Bull Seismol Soc Am 106(1):158–173

Bommer JJ, Dost B, Edwards B, Kruiver PP, Ntinalexis M, Rodriguez-Marek A, Stafford PJ, van Elk J (2017a) Developing a model for the prediction of ground motions due to earthquakes in the Groningen gas field. Neth J Geosci 96(5):203–213

Bommer JJ, Stafford PJ, Edwards B, Dost B, van Dedem E, Rodriguez-Marek A, Kruiver P, van Elk J, Doornhof D, Ntinalexis M (2017b) Framework for a ground-motion model for induced seismic hazard and risk analysis in the Groningen gas field, the Netherlands. Earthquake Spectra 33(2):481–498

Boore DM, Bommer JJ (2005) Processing strong-motion accelerograms: needs, options and consequences. Soil Dyn Earthq Eng 25(2):93–115

Bora SS, Scherbaum F, Kuehn N, Stafford P (2016) On the relationship between Fourier and response spectra: implications for the adjustment of empirical ground-motion prediction equations (GMPEs). Bull Seismol Soc Am 106(3):1235–1253

Bourne SJ, Oates SJ, Bommer JJ, Dost B, Van Elk J, Doornhof D (2015) A Monte Carlo Method for Probabilistic Hazard Assessment of Induced Seismicity due to Conventional Natural Gas Production. Bull Seismol Soc Am 105(3):1721–1738

Campman X, Behn P, Faber K (2016) Sensor density or sensor sensitivity? Lead Edge 35(7):578–585

Crowley H, Polidoro B, Pinho R, van Elk J (2017) Framework for developing fragility and consequence models for local personal risk. Earthquake Spectra 33(4):1325–1345

Crowley H, Pinho R, van Elk J, Uilenreef J (2019) Probabilistic damage assessment of buildings due to induced seismicity. Bull Earthq Eng 17(8):4495–4516. https://doi.org/10.1007/s10518-018-0462-1

Dost B, Ruigrok E, Spetzler J (2017) Development of seismicity and probabilistic hazard assessment for the Groningen gas field. Neth J Geosci 96(5):235–245

Dost B, Edwards B, Bommer JJ (2018) The relationship between M and M_L: A review and application to induced seismicity in the Groningen gas field, the Netherlands. Seismol Res Lett 89(3):1062–1074

Hofman, L. J., Ruigrok, E., Dost, B., & Paulssen, H. (2017). A shallow seismicvelocity model for the Groningen area in the Netherlands. Journal of GeophysicalResearch: Solid Earth, 122, 8035–8050. https://doi.org/10.1002/2017JB014419

Dost B, Edwards B, Bommer JJ (2019) Erratum to "The relationship between M and M_L: A review and application to induced seismicity in the Groningen gas field, the Netherlands". Seismological Research Letters, *in print*

Douglas J, Boore DM (2010) High-frequency filtering of strong-motion records. Bull Earthq Eng 9(2):395–409

Edwards B, Zurek B, van Dedem E, Stafford PJ, Oates S, van Elk J, Bommer JJ (2019) Simulations for the development of a ground motion model for induced seismicity in the Groningen gas field, The Netherlands. Bull Earthq Eng 17(8):4441–4456. https://doi.org/10.1007/s10518-018-0479-5

Graziotti F, Penna A, Magenes G (2018) A comprehensive in-situ and laboratory testing programme supporting seismic risk analysis of URM buildings subjected to induced earthquakes. Bulletin of Earthquake Engineering 17(8):4575–4599. https://doi.org/10.1007/s10518-018-0478-6

Green RA, Bommer JJ, Rodriguez-Marek A, Maurer BW, Stafford PJ, Edwards B, Kruiver PP, De Lange G, Van Elk J (2019) Addressing limitations in existing 'simplified' liquefaction triggering evaluation procedures: application to induced seismicity in the Groningen gas field. Bull Earthq Eng 17(8):4539–4557. https://doi.org/10.1007/s10518-018-0489-3

Kallioras S, Correia AA, Marques AI, Bernardo V, Candeias PX, Graziotti F (2019) LNEC-BUILD3: An incremental shake-table test on a Dutch URM detached house with chimneys. EUCENTRE Technical Report EUC203/2018U, European Centre for Training and Research in Earthquake Engineering, Pavia, Italy. Available at www.eucentre.it/nam-project

Konno K, Ohmachi T (1998) Ground-motion characteristics estimated from spectral ratio between horizontal and vertical

components of microtremor. Bull Seismol Soc Am 88(1): 228–241

Kruiver PP, van Dedem E, Romijn R, de Lange G, Korff M, Stafleu J, Gunnink JL, Rodriguez-Marek A, Bommer JJ, van Elk J, Doornhof D. An integrated shear-wave velocity model for the Groningen gas field, The Netherlands. Bulletin of Earthquake Engineering. 2017 Sep 1;15(9):3555-80.

Noorlandt R, Kruiver PP, de Kleine MP, Karaoulis M, de Lange G, Di Matteo A, von Ketelhodt J, Ruigrok E, Edwards B, Rodriguez-Marek A, Bommer JJ (2018) Characterisation of ground motion recording stations in the Groningen gas field. J Seismol 22(3):605–623

Rodriguez-Marek A, Kruiver PP, Meijers P, Bommer JJ, Dost B, van Elk J, Doornhof D (2017) A Regional Site-Response Model for the Groningen Gas FieldA Regional Site-Response Model for the Groningen Gas Field. Bull Seismol Soc Am 107(5):2067–2077

SBR (2002) Schade aan gebouwen meet-en beoordingsrichtlijn, Deel A 38 pp.

Spica ZJ, Perton M, Nakata N, Liu X, Beroza GC (2017) Site characterization at Groningen gas field area through joint surface-borehole H/V analysis. Geophys J Int 212(1):412–421

Spica ZJ, Nakata N, Liu X, Campman X, Tang Z, Beroza GC (2018) The ambient seismic field at Groningen gas field: An overview from the surface to reservoir depth. Seismol Res Lett 89(4):1450–1466

Stafford PJ, Zurek BD, Ntinalexis M, Bommer JJ (2019) Extensions to the Groningen ground-motion model for seismic risk calculations: component-to-component variability and spatial correlation. Bull Earthq Eng 17(8):4417–4439. https://doi.org/10.1007/s10518-018-0425-6

Tomassetti U, Correia AA, Candeias PX, Graziotti F, Costa AC (2019) Two-way bending out-of-plane collapse of a full-scale URM building tested on a shake table. Bull Earthq Eng 17(4):2165–2198

van Elk J, Doornhof D, Bommer JJ, Bourne SJ, Oates SJ, Pinho R, Crowley H (2017) Hazard and risk assessments for induced seismicity in Groningen. Neth J Geosci 96(5):259–269

van Elk J, Bourne SJ, Oates SJ, Bommer JJ, Pinho R, Crowley H (2019) A probabilistic model to evaluate options for mitigating induced seismic risk. Earthquake Spectra 35(2):537–564

Yudistra T, Paulssen H, Trampert J (2017) The crustal structure beneath TheNetherlands derived from ambient seismic noise. Tectonophysics 721: 361-371